Endothelium is required for the promotion of interrenal morphogenetic movement during early zebrafish development

Yi-Wen Liu [a,*], Lin Guo [b]

[a] Department of Life Science, Tunghai University, Taichung 40704, Taiwan R.O.C.
[b] Laboratory of Functional Genomics, Institute of Molecular and Cell Biology, Proteos, Singapore

Abstract

The adrenal cortex has a complex vasculature that is essential for growth, tissue maintenance, and access of secreted steroids to the bloodstream. However, the interaction between vasculature and adrenal cortex during early organogenesis remains largely unclear. In this study, we focused on the zebrafish counterpart of adrenal cortex, interrenal tissue, to explore the possible role of endothelium in the development of steroidogenic tissues. The ontogeny of interrenal tissue was found to be tightly associated with the endothelial cells (ECs) that constitute the axial vessels. The early interrenal primordia emerge as two clusters of cells that migrate centrally and converge at the midline, whereas the central convergence was abrogated in the avascular *cloche* (*clo*) mutant. Neither loss of blood circulation nor perturbations of vessel assembly could account for the interrenal convergence defect, implying a role of endothelial signaling prior to the formation of axial blood vessels. Moreover, as the absence of trunk endothelium in *clo* mutant was rescued by the forced expression of SCL, the interrenal fusion defect could be alleviated. We thus conclude that endothelial signaling is involved in the morphogenetic movement of early interrenal tissue.
© 2006 Elsevier Inc. All rights reserved.

Keywords: Adrenal; Interrenal; Endothelium; Steroidogenic; *cloche*; Zebrafish; Morphogenetic movement

Introduction

Endothelium has been discovered to communicate with organ tissues and provide inductive signals for organ development (reviewed in Cleaver and Melton, 2003; Nikolova and Lammert, 2003). For example, ECs promote the outgrowth and mesenchyme invasion of liver bud from hepatic endoderm, in an explant system, prior to the full formation of vasculature (Matsumoto et al., 2001). In the adult liver, selective activation of VEGF receptor 1 in the sinusoidal ECs leads to secretion of cytokines such as hepatocyte growth factor that stimulates hepatocyte proliferation (LeCouter et al., 2003). Also, the induction of dorsal pancreas is regulated by the ECs of aorta, which involves the activation of crucial pancreatic transcription factor Ptf1a (Lammert et al., 2001; Yoshitomi and Zaret, 2004). Among all the other organs that could be regulated by similar EC-related mechanisms, endocrine organs are of particular interest due to

their intimate dependence on blood circulation. Thus it would be intriguing to explore how signals from the developing vessels are shaping the morphology and function of endocrine organs.

The adrenal gland is comprised of an outer cortex, which synthesizes steroid hormones, and an inner medulla, which produces catecholamines. Both the adrenal cortex and medulla are highly vascularized, which is thought to be important for the development as well as secretory functions of adrenal gland. The dense distribution of vasculature in adrenal cortex requires the existence of an angiogenic molecule, endocrine gland VEGF (EG-VEGF), which is specifically expressed at steroidogenic tissues and is mitogenic as well as morphogenic for the ECs that populate the adrenal cortex (LeCouter et al., 2001). Interestingly, signals from endothelium have been identified as modulating certain differentiation events of the adrenal gland. For example, EC signals derived from adrenal capillary are able to regulate aldosterone release from steroidogenic zona glomerulosa, as revealed by coculture studies (Rosolowsky et al., 1999; Hanke and Campbell, 2000). Furthermore, cocultures of adrenal–medulla derived cell line PC12 with adrenal medulla ECs lead to

* Corresponding author. Fax: +886 4 2359 0296.
  E-mail address: dlslys@thu.edu.tw (Y.-W. Liu).

chromaffin-like differentiation of PC12 cells (Mizrachi et al., 1990). Beyond these functions in promoting endocrine differentiation and release, the role of endothelium in the early morphogenesis of adrenal gland has however remained unclear.

Zebrafish has matured into a valuable model for studying organogenesis such as the cardiovascular and digestive systems, since its embryos are amenable to molecular manipulations and genetic dissections. It has been utilized for studying the genetic determinants in the development of the embryonic kidney, the pronephros (reviewed in Drummond, 2003, 2005). Recently, an orphan nuclear receptor, ff1b, was identified to mark the ontogeny of interrenal tissue, the counterpart of mammalian adrenal cortex (Chai et al., 2003; Hsu et al., 2003), which leads to the possibilities of applying zebrafish model to the mechanistic studies of congenital adrenal abnormalities. The zebrafish interrenal organ is located within the head kidney, and its development parallels temporally and spatially that of the pronephros (Hsu et al., 2003). The interrenal and pronephric tissues, both derived from intermediate mesoderm, are distinct groups of cells in close proximity to each other, and both undergo central migration followed by fusion. Temporally, the fusion of bilateral interrenal primordia precedes the central assembly of pronephros. Morphogenetic movement of pronephros but not interrenal tissues is perturbed in notochord and sonic hedgehog mutants, suggesting that interrenal and pronephric cells receive different signals as migratory cues. The midline assembly of zebrafish pronephros is dependent on the expression of matrix metalloproteinase-2 regulated by hemodynamic force (Serluca et al., 2002). Furthermore, ECs are essential for the maturation of glomerular basement membrane in the developing pronephros (Majumdar and Drummond, 1999). It is thus of interest to explore how the interrenal organ would interact with ECs and the nascent vasculature, while the interrenal primordia are originated from the pronephric field.

Zebrafish embryo does not require blood to transport oxygen, and can develop up to at least 5 days post-fertilization (dpf) without circulation, making it an ideal system for genetic dissections of early endothelial development (Stainier et al., 1996; Davidson and Zon, 2004). Moreover, an array of cardiovascular mutants, in conjunction with organ-specific transgenic reporter lines, provides substantial opportunity for studying the role of endothelial signaling in either tissue or organ formation. Notably, the clo mutant is a powerful tool for analyzing the requirement of endothelium in various developmental processes, owing to the facts that its phenotypes are strikingly similar to those observed with Flk-1-deficient mice (Shalaby et al., 1995, 1997; Stainier et al., 1995). clo is required by both the endothelial and blood lineages at an early stage, suggesting a role in either the formation or maintenance of the hemagioblasts. The clo mutation leads to the loss of endocardium and most ECs, while a small population of poorly-differentiated ECs are still present in the lower trunk and tail vessels (Liao et al., 1997). Intriguingly, as endothelium is essential for directing the liver and pancreas budding processes in early mouse embryo, the absence of trunk endothelium in clo does not lead to significant perturbation in either liver or pancreas organogenesis (Field et al., 2003a,b). The discrepancy may arise from the species-specific differences in endodermal morphogenesis, or in the requirement of inductive signals (Cleaver and Melton, 2003). Nevertheless, clo remains an interesting tool for studying how the inductive properties of EC-derived signals are involved in other aspects of developmental processes, such as interrenal organogenesis.

This study sought to investigate the involvement of ECs in the steroidogenic component of early interrenal organ. By checking both ff1b expressions and 3β-Hsd enzymatic activities in the clo mutant embryo, we demonstrate that the presence of ECs is required for the convergence of bilateral interrenal promordia occurring shortly after interrenal specification. We show evidences that argue for an inductive role of endothelium, independent of either vessel formation or circulation, in the early interrenal morphogenetic movement. Also, although early interrenal primordia are originated from the pronephric field, the ECs that guide interrenal central migration are distinct from those invading the pronephric glomerulus. This study suggests that EC-derived paracrine factor(s) are essential in mediating the morphogenesis of steroidogenic tissues, at a stage well before the onset of endocrine function.

Materials and methods

Zebrafish strains and maintenance

Zebrafish (Danio rerio) were raised according to standard protocols (Westerfield, 2000). Embryos were obtained by natural spawning and cultured in embryo medium at 28.5°C. Staging of the embryos was carried out as previously described (Kimmel et al., 1995). Embryos to be used for histological analyses were treated with phenylthiourea (0.03%; Sigma) from 22 h post-fertilization (hpf) to inhibit melanin pigment formation. The $Tg(fli1:EGFP)^{Y1}$ line was obtained from the Zebrafish International Resource Center (Eugene, OR). The clo^{m39} mutant and $Tg(flk1:EGFP)^{s843}$ lines were obtained from Didier Stainier (San Francisco, CA).

Whole-mount in-situ hybridization

Whole-mount in-situ hybridization (ISH) was performed as described with minor modifications (Liu et al., 2003). Digoxigenin-labeled riboprobes were synthesized from plasmids containing cDNAs for flk1, wt1 and dβh. flk1 plasmid was linearized with NotI and transcribed with T7 RNA polymerase. wt1 plasmid was linearized with BamHI and transcribed with T7 RNA polymerase. dβh plasmid was linearized with NcoI and transcribed with Sp6 RNA polymerase. Fluorescein-labeled riboprobes were synthesized from SalI linearized ff1b plasmids and transcribed with T7 RNA polymerase. DIG-labeled riboprobes were detected with alkaline phosphatase conjugated anti-DIG antibody (Roche) while fluorescein-labeled probes were detected by alkaline phosphatase conjugated anti-fluorescein antibody (Roche). Visualization was performed either with NBT/BCIP (Promega), with BCIP/TNBT (Chemicon), or with Fast Red (Roche). For two-color in-situ hybridization, inactivation of the first antibody was performed by heating the stained embryos at 65°C for 30 min. Stained embryos were post-fixed in 4% paraformaldehyde (PFA) in PBS and washed in PBS supplemented with 1% of Triton X 100 (PBST). This was followed by tissue clarification in 50% glycerol in PBS. Specimens were mounted on glass slides and photographed under Nomaski optics on an Olympus BX51 microscope system.

Histology and microscopy

Histochemical staining for 3β-Hydroxysteroid dehydrogenase/Δ5-Δ4-isomerase (3β-Hsd) was performed on whole embryos using a protocol adapted from Levy's method as previously described (Grassi Milano et al., 1997).

Embryos were fixed for 1 h at RT in 4% PFA/PBS and washed twice with PBST. Chromogenic reaction was carried out at RT for overnight in staining solution containing 0.1 mg/ml etiocholan-3β-ol-17-one as substrate, 0.2 mg/ml NAD, 0.1 mg/ml of nicotinamide, and 0.1 mg/ml of nitroblue tetrazolium (Promega) in PBST. Staining reactions were terminated by washing in PBST. Chemicals were from Sigma unless otherwise stated. For simultaneous analysis of interrenal steroidogenic activity and endothelial GFP fluorescence, 3β-Hsd staining signals were captured using transmitted light, while the fluorescent signals were captured with Argon 488-nm laser connected to a Zeiss Axioplan II microscope equipped with LSM510 (Carl Zeiss Inc). The images were merged using the LSM 5 image browser software.

Diaminofluorene (DAF) staining was performed to detect the activity of hemoglobin peroxidase (modified from Weinstein et al., 1996). Embryos were fixed for 1 h at RT, washed 3 times with PBST, and preincubated in DAF staining solution (0.01% DAF, 200 mM Tris, pH 7.0, 0.05% Tween-20) for 1 h at RT in the dark. Hydrogen peroxide was added to a final concentration of 0.3%, and the embryos were incubated for a further 20 min. The reactions were terminated by washing in PBST. The images of blood cells in either DAF-stained or unstained whole-mount embryos were photographed under Nomarski optics.

Microinjection of morpholino oligonucleotides and plasmids

Morpholino oligonucleotides (MO) were synthesized at Genetools LLC. A 2 mM stock solution was prepared by dissolving lyophilized MO powder in 1 × Danieau solution, before further dilution into the required concentrations for microinjection. The nucleotide sequences of the *tnnt2*MO, *vegf*MO, *grl*MO, *scl* E1/IMO *scl* E2/IMO and STD-MO are 5′-CAT GTT TGC TCT GAT CTG ACA CGC A-3′ (Sehnert et al., 2002), 5′-GTA TCA AAT AAA

CAA CCA AGT TCA T-3′ (Nasevicius et al., 2000), 5′-CGC GCA GGT ACA GAC ACC AAA AAC T-3′ (Zhong et al., 2001), 5′-GCG GCG TTA CCT GTT AAT AGT GGC G-3′ (Dooley et al., 2005), 5′-AAT GCT CTT ACC ATC GTT GAT TTC-3′ (Dooley et al., 2005) and 5′-CCT CTT ACC TCA GTT ACA ATT TAT A-3′, respectively. Zebrafish *scl* full-length cDNA clone (IMAGE ID: 6964750) was obtained from Open Biosystems and subcloned into pCS2+ expression plasmid. MO- or plasmid-containing solutions (~ 2.3 nl) were injected into one- or two-cell stage embryos using a Nanoject injector (Drummond).

Results

ECs are in close proximity to early interrenal cells during and after the central migration and convergence of bilateral interrenal primordia

To explore the association of interrenal primordia and vasculature in the zebrafish embryo, the expression patterns of both *ff1b* and *flk1* were detected by whole-mount ISH. The expression of *ff1b* transcripts, marking the ontogeny of interrenal tissue, initiates as early as 22–24 hpf while the interrenal primordia are not yet committed to steroidogenesis (Chai et al., 2003; Hsu et al., 2003). Consistent with the previous studies, the early interrenal tissues were detected to emerge as two symmetric clusters of *ff1b*-expressing cells across the midline (Figs. 1A–C), which then underwent central
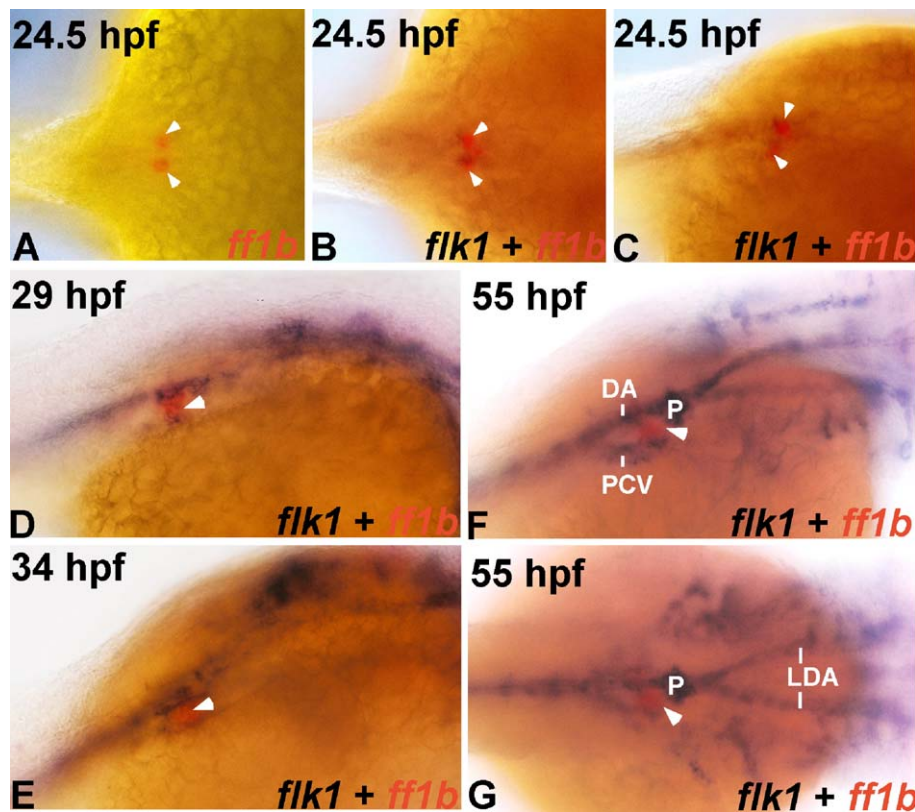

Fig. 1. Spatial relationship between interrenal tissue and endothelium during early zebrafish development. Developing wild type embryos at 24.5 hpf (A–C), 29 hpf (D), 34 hpf (E) and 55 hpf (F, G) were subject to either single ISH for *ff1b* (red) (A), or double ISH for *flk1* (dark blue) and *ff1b* (red) (B–G). Panels A, B and G are dorsal views, while panels C–F are dorsolateral views of the trunk region. All panels are oriented with anterior to the right. The tight association between interrenal tissue and endothelium initiates before the convergence of interrenal primordia. DA, dorsal aorta; PCV, posterior cardinal vein; P, pronephros; LDA, lateral dorsal aortae. White arrowheads indicate the interrenal tissues.

fusion and was displaced right of the midline (Figs. 1D–G). *flk1* gene, encoding a receptor tyrosine kinase, marks the endothelial precursors in developing vasculature (Liao et al., 1997). It is interesting to note that two clusters of *flk1*-expressing angioblasts were associated with the bilateral interrenal primordia, respectively (Figs. 1B and C). No vessel-like structures seemed to be formed by the angioblasts adjacent to bilateral interrenal primordia. These interrenal tissue-associated ECs were apparently at the migratory state at 29 hpf (Fig. 2C),

suggesting their involvement in the process of axial vessel assembly.

After the convergence of interrenal primordia, the *ff1b*-expressing cell cluster remained closely associated with the *flk1*-expressing cells that marked developing midline vasculature including dorsal aorta, posterior cardinal vein as well as glomerular endothelium of pronephros (Figs. 1D–G). From 29 to 34 hpf, the cluster of *ff1b*-expressing cells was sandwiched between dorsal and ventral subsets of *flk1*-expressing ECs
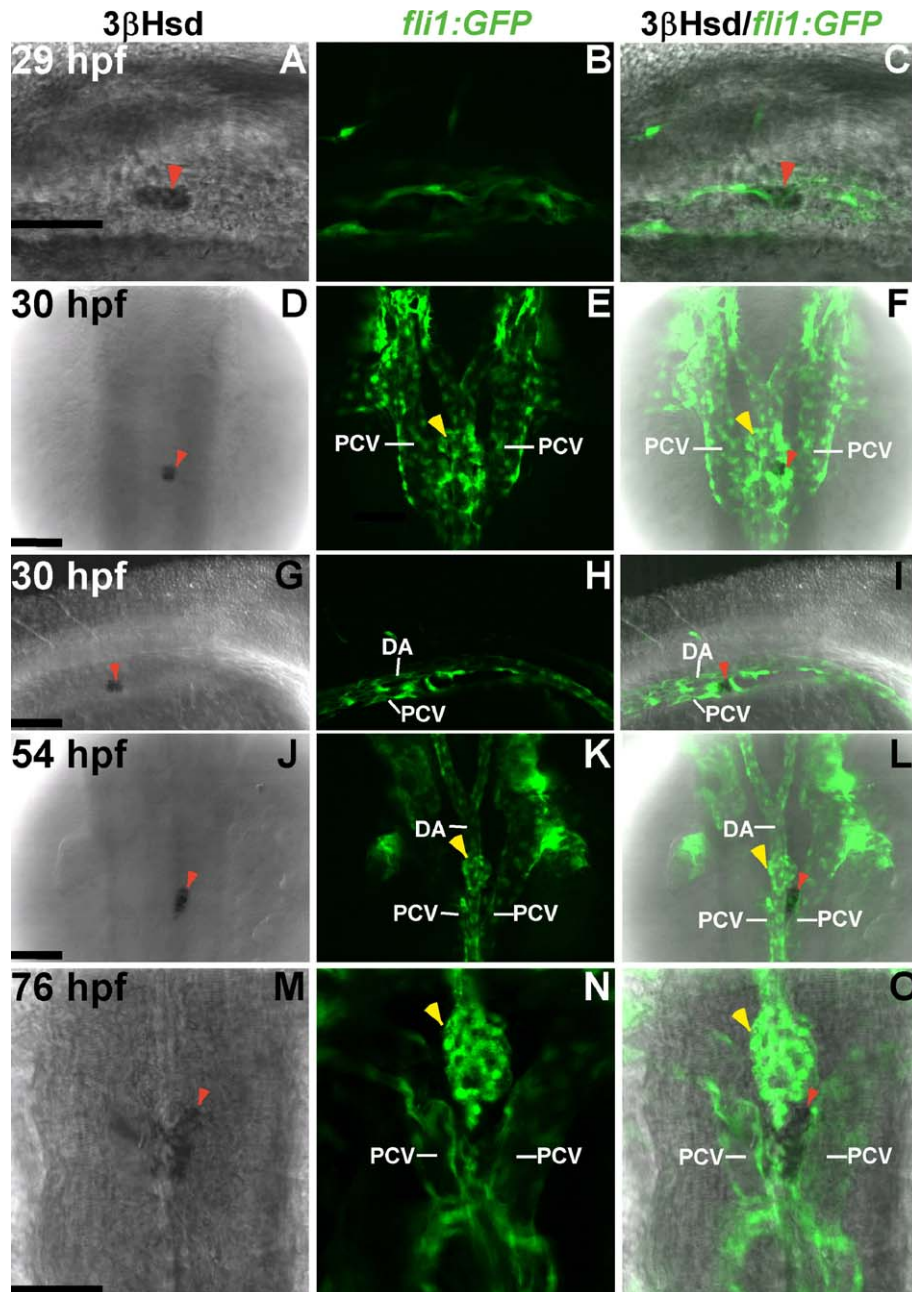

Fig. 2. Interaction of interrenal and endothelial cells as revealed in *Tg(fli1:EGFP)*[Y1] transgenic zebrafish. Single confocal sections showing the interrenal tissues as stained by 3β-Hsd activity assay (left panel: A, D, G, J, M), and the neighboring ECs as labeled by green fluorescence (middle panel: B, E, H, K, N), of *Tg(fli1:EGFP)*[Y1] embryos while staged at 29 hpf (A–C), 30 hpf (D–I), 54 hpf (J–L) and 76 hpf (M–O), respectively. The merged images of 3β-Hsd activity and GFP are shown in the right panel (C, F, I, L, O). Panels A–C and panels G–I are lateral views with anterior oriented to the right. Panels D–F and panels J–O are dorsal views with anterior oriented to the top. The interrenal cells are in close contact with ECs that are engaged in axial vessel assembly. DA, dorsal aorta; PCV, posterior cardinal vein. Red arrowheads indicate interrenal tissues, while yellow arrowheads indicate glomeruli. Scale bar, 50 μM.

which appeared to form part of the dorsal aorta and posterior cardinal vein, respectively (Figs. 1D, E). At 55 hpf, the developing pronephric glomerulus was situated immediately caudal to the radix of aorta (Figs. 1F, G). Further posteriorly, the interrenal tissue lay in closely proximity to the glomerulus, with the cell cluster juxtaposed between dorsal aorta and right posterior cardinal vein, either from a dorsal lateral or dorsal top view. In summary, the expressions of *ff1b* and *flk1* in zebrafish embryo revealed a tight association of interrenal tissue with ECs, which occurred as early as the specification of interrenal tissues while the central convergence of bilateral primordia was not yet completed.

The interactions between steroidogenic and endothelial cells in development

The specification and central convergence of interrenal primordia are followed by the initiation of steroidogenic enzyme expressions at around 28.5 hpf (Chai et al., 2003; Hsu et al., 2003). Consistent with the results demonstrated in Fig. 1, the onset of steroidogenesis at embryonic interrenal tissue was found to be tightly associated with ECs that constitute developing midline vasculature (Fig. 2). To visualize the steroidogenic cells, chromogenic enzymatic activity assays of 3β−Hsd were performed on various stages of *Tg(fli1: EGFP)^{y1}* embryos. The GFP fluorescence of *fli1*, an ETS-domain transcription factor gene, allows dynamic recapitulation of embryonic vasculature in vivo (Lawson and Weinstein, 2002). At 29 hpf, some of the trunk ECs apparently at migratory state were intimately attached to the surface of steroidogenic cell cluster (Figs. 2A–C). Shortly after 29 hpf, the steroidogenic cell cluster was encapsulated by the ECs that were forming axial vessels (Figs. 2D–I). From 29 hpf onwards till 36 hpf, the interrenal primordium is located beneath the third somite and immediately dorsal to the yolk sac (Chai et al., 2003; Liu et al., 2003). The dorsal view of 30 hpf embryo showed that the interrenal cell cluster was situated posterior to the pronephric glomerulus invaded by ECs, and anterior to the branching point of posterior cardinal vein (Figs. 2D–F). Part of the glomerular endothelium at right latero-posterior portion of pronephros appeared to lie upon the rostral end of interrenal tissue (Fig. 2F). The lateral view of 30 hpf embryo showed that the dorsal surface of interrenal tissue was overlaid by ECs of aorta, while the lateral as well as ventral surfaces were enveloped by ECs of axial vein (Figs. 2G–I).

Well after the initiation of axial vessel assembly and trunk circulation, the vascularization of pronephric glomerulus became evident at 54 hpf (Figs. 2K, L). At this stage, the interrenal tissue remained tightly surrounded by the neighboring axial vessels (Figs. 2J, L). Consistent with the results of ISH detecting *ff1b* transcripts, the 3β-Hsd-expressing cell cluster was juxtaposed between dorsal aorta and right posterior cardinal vein at 54 hpf, just cranial to where the posterior cardinal vein branches bilaterally. Along with the central assembly of blood vessels, the contour of steroidogenic interrenal tissue appeared to be delineated by the adjacent vessel walls, and the boundary between glomerular endothelium and interrenal cells was

evident at 54 hpf (Figs. 2K, L). Although individual angioblasts were attached to the interrenal tissue at this stage, no invagination of ECs was detected by our cryosection analysis (results not shown). The relative spatial relationship of steroidogenic interrenal tissue and glomerular endothelium, as detected by 3β-Hsd-positive and *fli1*-positive cells, respectively, essentially resembled that of *ff1b*- and *Wilm's tumor 1* (*wt1*)-expressing cells as detected by double-labeling ISH assays (Hsu et al., 2003).

At 76 hpf, the interrenal cell cluster expanded and extended across the midline (Figs. 2M–O). Concomitant with a decreased midline asymmetry, the interrenal tissue was displaced beneath the mid-ventral surface of dorsal aorta. Furthermore, the dorsal top view demonstrated that the interrenal tissue was in intimate contact with the caudal end of glomerular endothelium, and confined in-between the paired branches of posterior cardinal vein. Morphologically, the V-shape structure of interrenal tissue, as viewed dorsally, seemed to be defined by the surrounding endothelium. Moreover, the invagination of ECs into interrenal tissue was evident at this stage.

Throughout the process of morphogenesis that followed the onset of steroidogenesis, interrenal tissue was found to be tightly associated with developing vessels, which is consistent with the notion that vasculature is functionally required for the endocrine tissues. Also, the spatial relationship suggests the possibility of mutual signaling events between interrenal organ and vasculature during early zebrafish development.

Incomplete central convergence of interrenal primordia is detected in the EC-free trunk region of clo^{m39} mutant

To explore the role of endothelium in interrenal development, we examined the expression patterns of *ff1b* in the *clo^{m39}* mutant where trunk endothelium is completely absent. It is shown in Figs. 3A–D that the *ff1b* transcription at early interrenal tissue was not reduced, implying that the specification of interrenal organ does not require endothelium. However, the convergence of bilateral interrenal primordia was arrested in *clo^{m39}*, which might arise from a failure of central migration. In contrast, the pattern of *ff1b* expression at ventral hypothalamus was not perturbed in *clo^{m39}* as compared with wild-type siblings (Figs. 3E, F), indicating that the migration defects of *ff1b*-expressing tissues are interrenal-specific. By monitoring interrenal development using 3β-Hsd activity assays, the effect of *clo^{m39}* mutation on interrenal convergence was found to be persistent up to 77 hpf (Figs. 3G, H), with the interrenal primordia remaining symmetrically distributed across midline. Also, the synthesis of 3β-Hsd did not appear to be perturbed in the interrenal tissue of *clo^{m39}*. Collectively, it is implied that the migration defect might be due to the deficiency of specific signaling events, rather than to a delay of development. The penetrance of interrenal convergence defect was 88.2% among the homozygous *clo^{m39}* mutants (n of *clo^{m39−/−}* = 93), and was 2.2% among the wild type sibling controls (*n* = 279). The utilization of 3β-Hsd assay for detecting developing interrenal tissue however led to a 72.5% penetrance among the homozygous *clo^{m39}* mutants at 77 hpf (n of *clo^{m39}* = 51), and
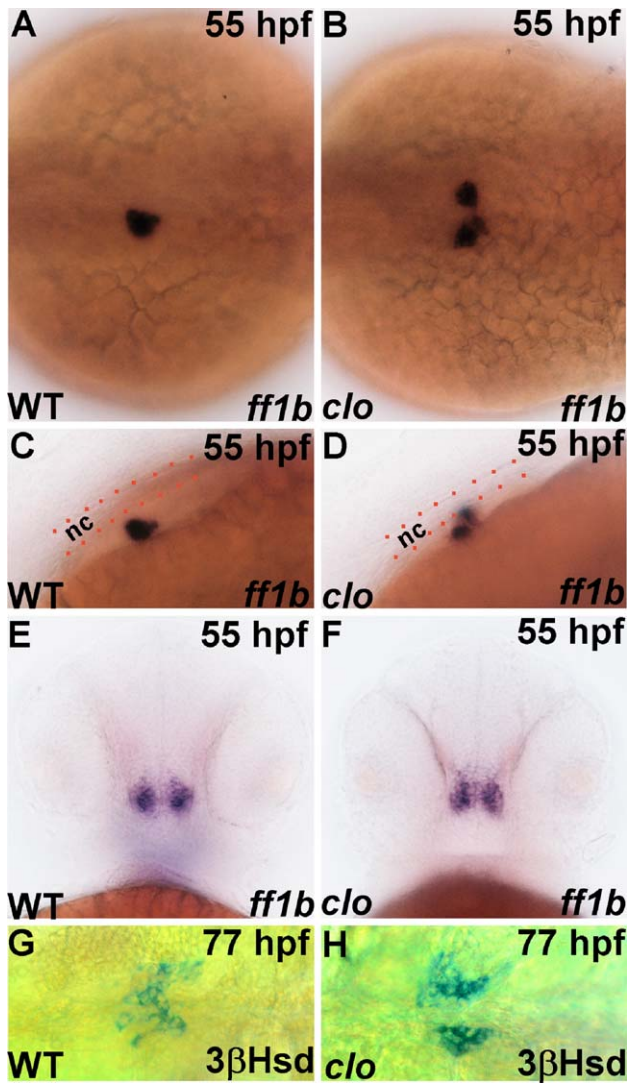
Fig. 3. *ff1b* expression and 3β-Hsd enzymatic activity in the *clo^m39* mutant and its wild type sibling. Embryos of *clo^m39* mutant (right panel: B, D, F, H) and its wild-type sibling (WT, left panel: A, C, E, G) were labeled by ISH for *ff1b* (dark blue) at 55 hpf (A–F), or by chromogenic detection of 3β-Hsd activity at 77 hpf (G, H). Panels A and B are dorsal views while panels C and D are dorsolateral views of embryos oriented with anterior to the right. Panels E and F are frontal views showing the *ff1b* expression in ventral hypothalamus. Panels G and H are ventral views of deyolked embryos oriented with anterior to the right. The central migration of interrenal tissue is arrested in *clo^m39*, resulting in persistent distribution of a pair of cell clusters on either side of notochord. Notochords (nc) dorsal to the interrenal tissues are outlined by red dots in panels C and D.

central merging at this stage (Fig. 4A), while the interrenal convergence had taken place earlier. The central migration of both pronephros and interrenal tissue was defective in *clo^m39* (Fig. 4B), with the relative localization of *wt1* and *ff1b* in trunk region resembling that observed in the 24 hpf wild type embryos. The migration defect of pronephric tissues in *clo^m39* is consistent with the previous study by Serluca et al. (2002) that the pronephric glomerular assembly at midline requires vascular flow.

Instead of being embedded in the center of adrenal cortex, the adrenomedullary cells are known to intermingle with the interrenal cells, to varying extent depending on the species, in the head kidney of teleosts (Grassi Milano et al., 1997). Teleostean chromaffin cells express Dopamine β-hydroxylase (DβH), which converts dopamine to noradrenaline (Reid et al., 1995; Grassi Milano et al., 1997). The gene expression pattern of *dβh* in the trunk region of 2 dpf zebrafish embryo reveals two major clusters of *dβh*-expressing cells, with one cluster tightly associated with *ff1b*-expressing cells (Chai et al., 2003). At 77 hpf, the dispersed clusters of *dβh*-expressing cells merged at midline and became intimately intermingled with the interrenal cells (Fig. 4C). In *clo^m39*, the merge of adrenomedulla cell clusters to midline was not perturbed, although there was an obvious decrease in the *dβh* transcripts (Fig. 4D). Whether the decrease of *dβh* expression indicates a reduced number or inhibited function of chromaffin cells remains to be studied. Nevertheless, the results clearly show that the central migration of chromaffin cells was independent of the existence of endothelium at trunk midline. It remains unclear whether the defective morphology of chromaffin cell cluster in *clo^m39* was due to the endothelium deficiency. Another possible cause of the chromaffin tissue defect in *clo^m39* might be a loss of interaction between interrenal and chromaffin cells, resulting from the disrupted assembly of interrenal tissues to midline. The latter possibility is supported by a previous study of Sf1 mutant mice, where the absence of adrenal cortex affects neither the determination of chromaffin cell fate nor their proper assembly to the suprarenal region, while the number of chromaffin cells is significantly reduced (Gut et al., 2005). However, the respective effects of endothelium- vs. interrenal-derived signals, on the morphogenesis of chromaffin tissue, remain to be dissected.

The assembly of pronephric glomerulus, but not interrenal tissue, is perturbed in the absence of either blood flow or vascular remodeling

Since circulation is not established in *clo^m39* mutant, it is necessary to verify whether the interrenal morphogenetic defect in *clo^m39* was due to a lack of blood flow. To address this issue, antisense morpholino oligos against *cardiac troponin T2* (*tnnt2*) gene (Bartman et al., 2004; Sehnert et al., 2002) were administered to 1–2 cell embryos of *Tg(fli1:EGFP)^y1* for the inhibition of heartbeat, which led to the absence of blood flow. *tnnt2* is expressed in a cardiac-specific manner and mutated in the *silent heart* (*sil*) mutant, where a non-contractile heart phenotype with severely defective assembly of sarcomere is displayed (Sehnert et al., 2002). All of the *tnnt2* morphants, as
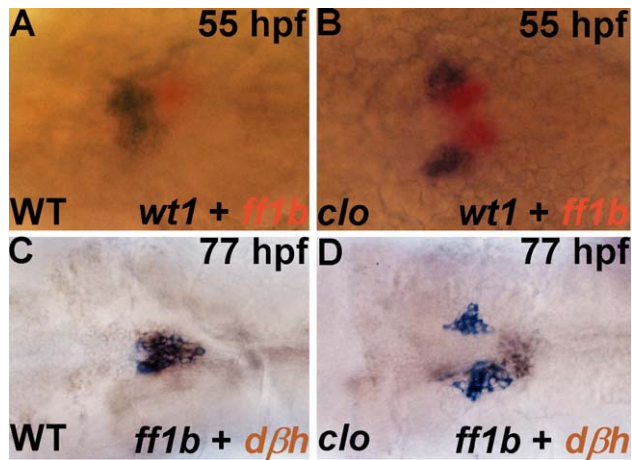
a 2.6% penetrance among wild type sibling controls (*n* = 152). The lower penetrance of the interrenal migration phenotype as revealed by 3β-Hsd staining might reflect the heterogeneity of steroidogenic potential for bilateral interrenal cell clusters, while their merging was arrested in *clo^m39*.

While the convergence of interrenal tissue was arrested in *clo^m39*, the pronephros displayed a parallel central migration defect. Double ISH assays detecting pronephros and interrenal tissues, by the probes for *wt1* and *ff1b*, respectively, were performed on *clo^m39* and its wild-type sibling at 55 hpf (Figs. 4A, B). Consistent with the previous results by Hsu et al. (2003), the bilateral *wt1*-expressing primordia were close to

Fig. 4. Migration of pronephros and chromaffin tissues in the *clo^{m39}* mutant and its wild type sibling. Pronephros and interrenal tissues in *clo^{m39}* (B) and its wild type sibling (WT, A) at 55 hpf were detected by double ISH for *wt1* (dark brown) and *ff1b* (red), respectively. Interrenal and chromaffin tissues in *clo^{m39}* (D) and its wild type sibling (C) at 77 hpf were detected by double ISH for *ff1b* (blue) and *dβh* (dark brown), respectively. All panels are dorsal views oriented with anterior to the left. The central merge of pronephric primordia is defective in *clo^{m39}*, while the migration and coalescence of chromaffin tissues are unperturbed.

injected at the dosage of 1 pmole per embryo, displayed complete absence of heartbeat as well as circulation at 55 hpf (*n* = 246). The glomerular assembly of pronephros was defective in *tnnt2* morphants, while the endothelial invasion apparently unaffected (Figs. 5E, F), which is consistent with the

results by Serluca et al. (2002) that glomerular assembly at midline was disrupted in *sil* embryo as detected by *wt1* expression. Although there was severe disruption of circulation as well as pronephros phenotypes in *tnnt2* morphants, 98% of the injected embryos displayed normal convergence of interrenal primordia (Figs. 5D–F), with the ratio not significantly varying from that derived from the control embryos injected with STD-MO (1/184) which produced no visible cardiovascular phenotypes. In the *tnnt2* morphant, the coalesced cluster of interrenal tissue was juxtaposed between the right lobe of unfused pronephric primordia and the right posterior cardinal vein. The results thus rule out the possibility of hemodynamic force being involved in the morphogenetic movements of early interrenal tissues. Also, the central migration of interrenal primordia is not affected as the bilateral glomerular EC clusters do not assemble at midline, implying that the subset of ECs directing interrenal migration are distinct from the glomerular endothelium. Hence, differential guidance cues might be exerted by distinct populations of angioblasts which all migrate and assemble into axial vessels.

The disrupted assembly of pronephric glomerulus was also found while the angiogenesis was inhibited in developing zebrafish embryo by the injection of antisense morpholino oligos against *vegf-A* gene (*vegf*MO) (Fig. 6). Vegf-A has been shown to be required for angiogenesis and blood formation, but not for initial patterning of axial vasculature (Nasevicius et al., 2000). Also, the expression of *vegf* is generally independent of *clo* function, although the Vegf-A receptor *flk-1* acts downstream of *clo* in the endothelial differentiation (Liao et al.,
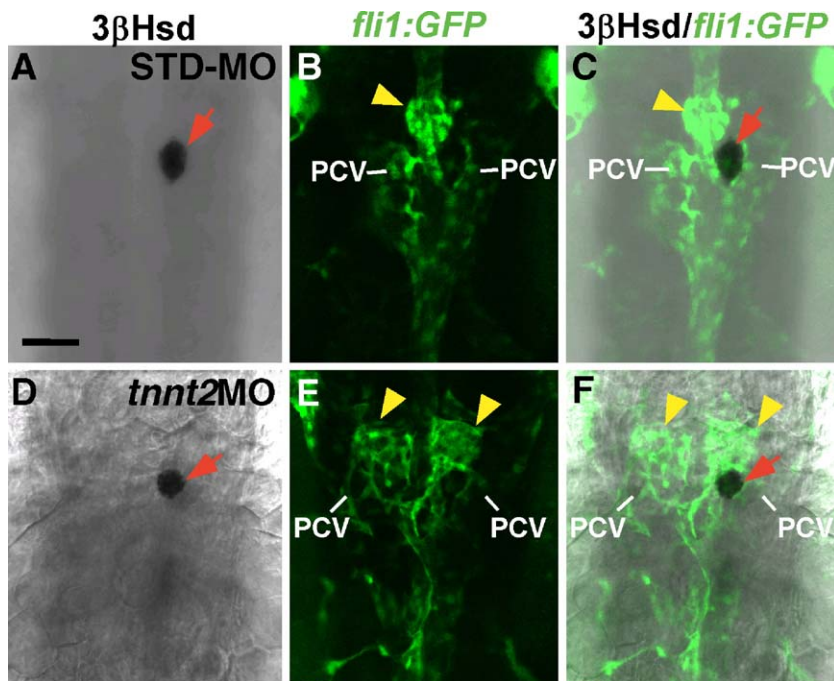

Fig. 5. Effects of *tnnt2* antisense morpholino injection on the interrenal tissue. Single confocal sections showing the interrenal tissues as detected by 3β-Hsd activity staining (left panel: A, D), and the neighboring ECs as labeled by green fluorescence (middle panel: B, E), of 56 hpf *Tg(fli1:EGFP)^{Y1}* embryos injected with STD-MO (A–C) and *tnnt2*MO (D–F), respectively. The merged images of 3β-Hsd activity and GFP are shown in the right panels C and F. All panels are dorsal views with anterior oriented to the top. The convergence of glomerular but not interrenal tissues is perturbed in *tnnt2* morphants. PCV, posterior cardinal vein. Red arrows indicate interrenal tissues, while yellow arrowheads indicate glomeruli. Scale bar, 50 μM.
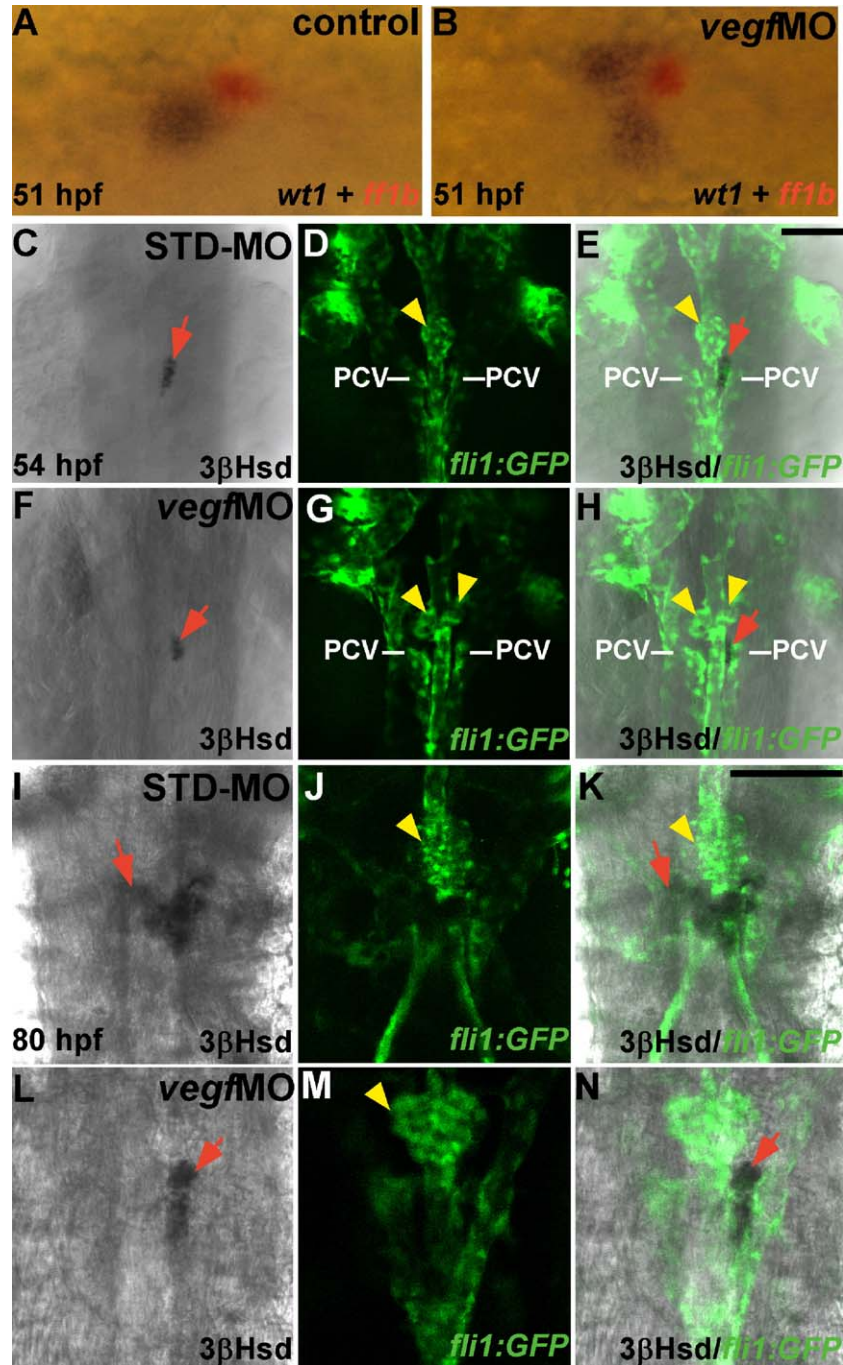
Fig. 6. Effects of *vegf-A* antisense morpholino injection on the interrenal tissue. (A, B) Dorsal views of uninjected control (A) and *vegf-A* morphant (B) embryos after double ISH for *wt1* (dark brown) and *ff1b* (red) at 51 hpf, oriented with anterior to the left. (C–N) Single confocal sections showing the dorsal views of interrenal tissues as detected by 3β-Hsd activity staining (C, F, I, L), and the neighboring ECs as labeled by green fluorescence (D, G, J, M), of 54 hpf (C–H) or 80 hpf (I–N) *Tg (fli1:EGFP)^{Y1}* embryos injected with STD-MO (C–E, I–K) and *vegf*MO (F–H, L–N), respectively and oriented with anterior to the top. The merged images of 3β-Hsd activity and GFP are shown in panels E, H, K and N. The convergence of pronephric but not interrenal tissues is perturbed in *vegf-A* morphants. PCV, posterior cardinal vein. Red arrows indicate interrenal tissues, while yellow arrowheads indicate glomeruli. Scale bar, 50 μM.

1997). More than 99% of the *vegf*MO-injected *Tg(fli1:EGFP)^{Y1}* embryos displayed characteristic phenotypes of pericardial enlargement and failure of RBC formation, as well as inhibited angiogenesis as revealed by the perturbed formation of intersegmental vessels (*n* = 146, results not shown). Accompanying the angiogenetic defects, the central migration of pronephric tissues was disrupted in 91% of *vegf-A* morphants as

detected by ISH for *wt1* expression (53/58, Figs. 6A, B). Similar to the results with *tnnt2* morphants, the central migration and convergence of interrenal primordia was not affected while the glomerular assembly was perturbed in *vegf-A* morphants at 54 hpf, as compared with the STD-MO injected controls (Figs. 6C–H). Although the interrenal morphogenetic movement was not affected in *vegf-A* morphants, the growth and expansion of

interrenal primordium was apparently reduced as observed at 80 hpf (Figs. 6I–N), which seemed to be correlated with a poorly developed axial vascular system. We conclude from the results of both *tnnt2* and *vegf-A* morphants that neither blood circulation nor glomerular assembly was correlated with the convergence of interrenal primordia, indicating that the guiding signal might arise from those ECs involved in earlier events of axial vessel patterning.

The convergence of interrenal primordia is unaffected while the arterial assembly is disrupted

To test the hypothesis above, we further proceeded to explore whether the convergence of bilateral interrenal primordia was affected while the formation of axial vasculature was disrupted. The axial vessels are assembled by the central migration and coalescence of angioblasts in the trunk, while the differentiation of arterial and venous cells occurs prior to the vascular assembly and blood circulation. The establishment of trunk artery in zebrafish embryo requires *gridlock* (Zhong et al., 2000, 2001), a basic helix–loop–helix (bHLH) gene, while the coalescence of axial vein at midline was thought to be due to a general morphogenetic movement. Antisense morpholino oligos against *grl*

(*grl*MO) leads to the reduction of aorta in a dose-dependent manner, which was accompanied by an expansion of venous region (Zhong et al., 2001). To achieve an effective reduction effect of aorta, we injected *grl*MO into *Tg(fli1:EGFP)^{Y1}* embryos at a high dosage of 1.42 pmole per embryo. At 54 hpf, 76% of the *grl* morphants (336/442) appeared to display neither blood flow nor visible dorsal aorta (pictures from a representative *grl* morphant shown in Figs. 7E, F, K, L) as compared with STD-MO injected controls (Figs. 7B, C, H, I), while the rest showed remnants of the rostral part of dorsal aorta. Enlarged heart cavities were found in all of the *grl* morphants, which were characteristic of a perturbed cardiovascular system. Despite the severely compromised arterial assembly, normal convergence of interrenal primordia was found in 90% of *grl* morphants completely lacking dorsal aorta, and in 89% of the *grl* morphants with defective arterial assembly. The arterial cells overlaying the interrenal tissue were missing in *grl* morphants (Figs. 7K, L), while the venous region surrounding the interrenal tissue cluster appeared to be expanded in size. It remains unclear why the percentage of normal convergence phenotype in *grl* morphants was lower than STD-MO injected controls (98.3%, $n = 402$), and we speculate that the malformed venous structure in some of the *grl*
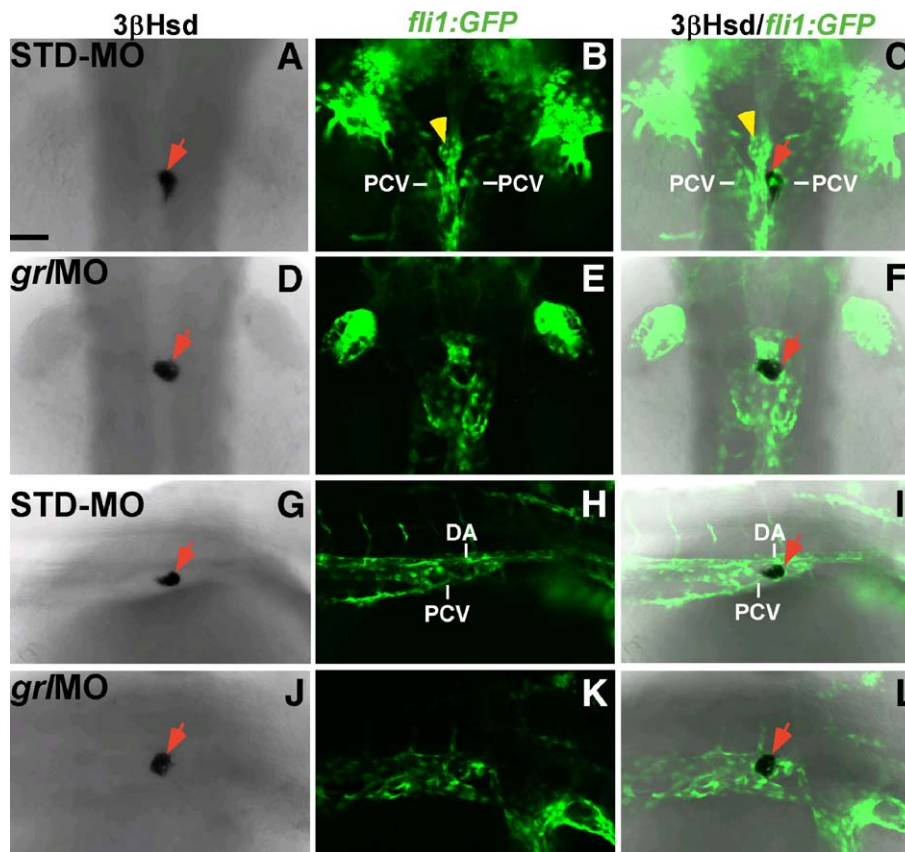

Fig. 7. Effects of *grl* antisense morpholino injection on the interrenal tissue and its neighboring vasculature. Single confocal sections showing the interrenal tissues as detected by 3β-Hsd activity staining (left panel: A, D, G, J), and the neighboring ECs as labeled by green fluorescence (middle panel: B, E, H, K), of 56 hpf *Tg(fli1: EGFP)^{Y1}* embryos injected with STD-MO (A–C, G–I) and *grl*MO (D–F, J–L), respectively. The merged images of 3β-Hsd activity staining and GFP are shown in the right panels C, F, I and L. Panels A–F are dorsal views with anterior oriented to the top, while panels G–L are dorsolateral views with anterior to the right. The disruption of dorsal aorta through injection of *grl* morpholino does not significantly perturb the interrenal convergence. DA, dorsal aorta; PCV, posterior cardinal vein. Red arrows indicate interrenal tissues, while yellow arrowheads indicate glomeruli. Scale bar, 50 μM.

morphants might affect the migration of interrenal primordia. Nevertheless, the results with *grl* morphants revealed that the central migration of interrenal primordia is not correlated with the establishment of trunk artery at midline. Consistently, previous studies have shown that the interrenal morphogenetic movements are essentially unaffected in both *no tail* and *floating head* mutants (Chai et al., 2003; Liu et al., 2003), while both display repressed formation of dorsal aorta which may be due to a deficiency in notochord-derived signals (Fouquet et al., 1997; Sumoy et al., 1997).

The convergence of interrenal primordia is normal in the absence of blood

Both blood and endothelial lineages are disrupted in *clo* in a combined and highly correlated fashion, arguing for the intimate interaction between blood and endothelium in development (Stainier et al., 1995; Parker and Stainier, 1999). Also, *clo* acts upstream of *scl*, a bHLH transcription factor involved in both hematopoietic and endothelial development. SCL is required at the stem cell level for the specification of all blood lineages (reviewed in Green, 1996; Shivdasani and Orkin, 1996). In zebrafish embryo, antisense morpholino oligos targeting against splice-donor sites of *scl* lead to the abrogation of blood lineages and the disruption of dorsal aorta (Dooley et al., 2005; Patterson et al., 2005). It is thus necessary to verify whether the blood deficiency in *clo*, apart from a parallel endothelial defect, would contribute to the failed convergence of interrenal tissue. To test this possibility, an equimolar mixture of *scl* E1/IMO and *scl* E2/IMO were co-injected into *Tg(fli1:EGFP)* embryos, at a final dosage of 1.2 pmole per embryo. The effectiveness of injected *scl*MOs at such dosage was validated by a complete loss of hemoglobin peroxidase activity in the DAF staining assay (Fig. 8B), as well as an absence of visible blood cells in unstained embryos (Fig. 8D). Among the *scl* morphants verified to contain no blood cells by 53 hpf ($n = 290$) through the microscopic observation of live embryos, 82.8% were found to be disrupted in the assembly of axial vessels (Figs. 8F, G), while more than 99% were normal in terms of the interrenal convergence at midline (Figs. 8E, G). The results clearly showed that the defects of blood lineage formation do not account for the interrenal migration phenotype in clo^{m39}.

The interrenal convergence defects in clo^{m39} can be alleviated while endothelium is partially rescued by the forced expression of SCL

The above experiments rule out the possibilities of either blood circulation or vascular formation being involved in directing the interrenal morphogenetic movement. It is thus
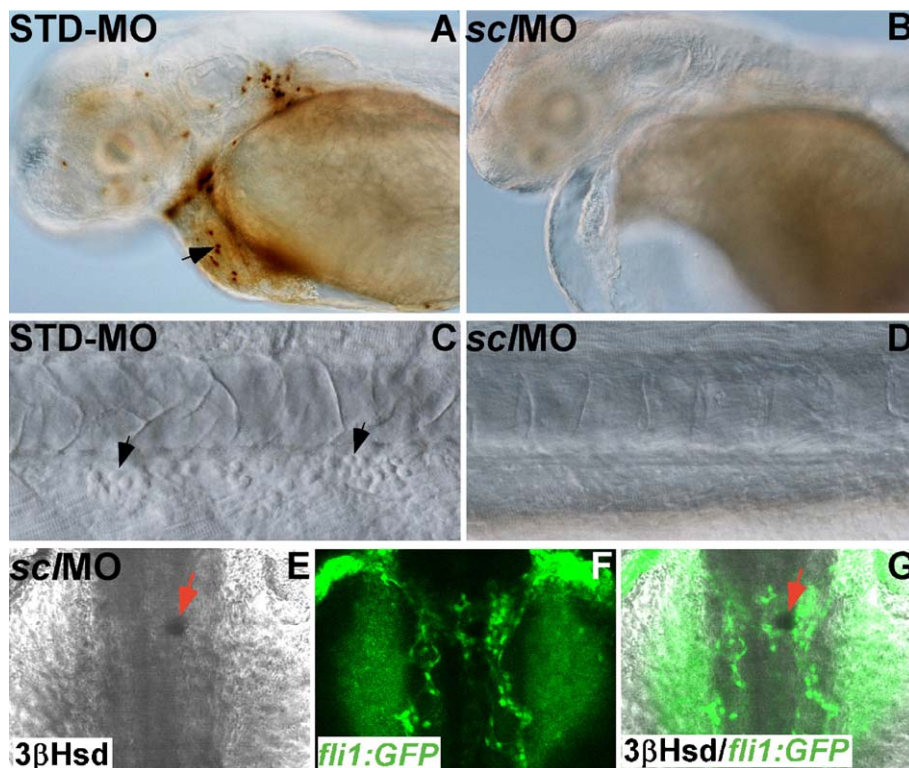

Fig. 8. Effects of *scl* antisense morpholino injection on the interrenal tissue. (A–D) Lateral views of embryos injected with STD-MO (A, C) and *scl*MO (B, D), respectively, harvested at 51 hpf, and subject to either DAF staining (A, B) or no staining (C, D) prior to Nomarski photomicroscopy. Blood cells are present in the anterior portion (A) and tail vessels (C) of STD-MO-injected embryos, but not detected in the *scl* morphants (B, D). (E–G) Single confocal sections showing the dorsal views of interrenal tissues as stained by 3β-Hsd activity assay (E), and neighboring ECs as labeled by green fluorescence (F), of 53 hpf *Tg(fli1:EGFP)^{Y1}* embryos injected with *scl*MOs. The merged images of 3β-Hsd activity and GFP are shown in panel G. Anterior is oriented to the left in panels A–D and to the top in panels E–G. The central convergence of interrenal tissues is not affected in *scl* morphants where blood cells are absent. Black arrows indicate blood cells, and red arrows indicate interrenal tissues.

Table 1
Rescue of endothelium and interrenal convergence in $Tg(flk1:EGFP)^{s843}$; clo^{m39} mutants by the injection of SCL expression plasmids

Embryo	Plasmid	$flk1$-EGFP near IR	Convergence of IR (by 3β-Hsd)	
			Normal	Defective
Mutant	cmv-SCL	Rescue (53)	39 (74%)	14 (26%)
		No rescue (140)	37 (26%)	103 (74%)
Wild type	cmv-SCL	Normal (577)	562 (97%)	15 (3%)
Mutant	cmv	Rescue (0)	0	0
		No rescue (41)	12 (29%)	29 (71%)
Wild type	cmv	Normal (121)	117 (97%)	4 (3%)

Summary of microinjection rescue experiments in $Tg(flk1:EGFP)^{s843}$; clo^{m39}. pCS2+ control (cmv) or pCS2+SCL expression (cmv-SCL) plasmids were microinjected into 1- to 2-cell-stage embryos from heterozygote pair-wise mating, and scored at 3 dpf. All of the homozygous clo^{m39} mutants (mutant) did not show detectable fluorescence at the trunk region. In contrast, the wild-type siblings of clo^{m39} (wild type), whether injected with cmv or with cmv-SCL plasmids, displayed normal $flk1$-promoter directed GFP fluorescence ($flk1$-EGFP) near the interrenal tissue (IR), as seen in the uninjected controls. The plasmid-injected mutant embryos displaying clear fluorescence near the IR region, with the pattern of axial vasculature as shown in Fig. 9H, were classified as "rescue"; while those showing faint or no fluorescence as "no rescue".

suggested that the signaling mediated by angioblasts prior to vessel formation might account for the migration of early interrenal cells toward midline. Based on this hypothesis, it is essential to verify whether the interrenal phenotype in clo^{m39} mutant reflects an autonomous function of clo at interrenal tissue, or is secondary to the absence of ECs. To address this issue, the trunk endothelium of clo^{m39} mutants was rescued by the injection of scl expression plasmids into a clo^{m39} strain which was crossed to $Tg(flk1:EGFP)^{s843}$ line for monitoring endothelial development. In $Tg(flk1:EGFP)^{s843}$, the GFP fluorescence driven by $flk1$ promoter is found in ECs that form nascent vasculature, whereas the fluorescent cells are completely absent in the trunk region of homozygous $Tg(flk1:EGFP)^{s843}$;clo embryos (Jin et al., 2005). The forced expression of SCL resulting from injection of scl plasmids has been shown to rescue the trunk endothelium and hematopoietic markers in clo (Liao et al., 1998; Porcher et al., 1999), although similar rescuing effects are not found while clo^{m39} is injected with scl mRNAs (Dooley et al., 2005). The results of the effects of scl-plasmid injections on trunk endothelium and interrenal morphology of homozygous $Tg(flk1:EGFP)^{s843}$;clo^{m39}, as
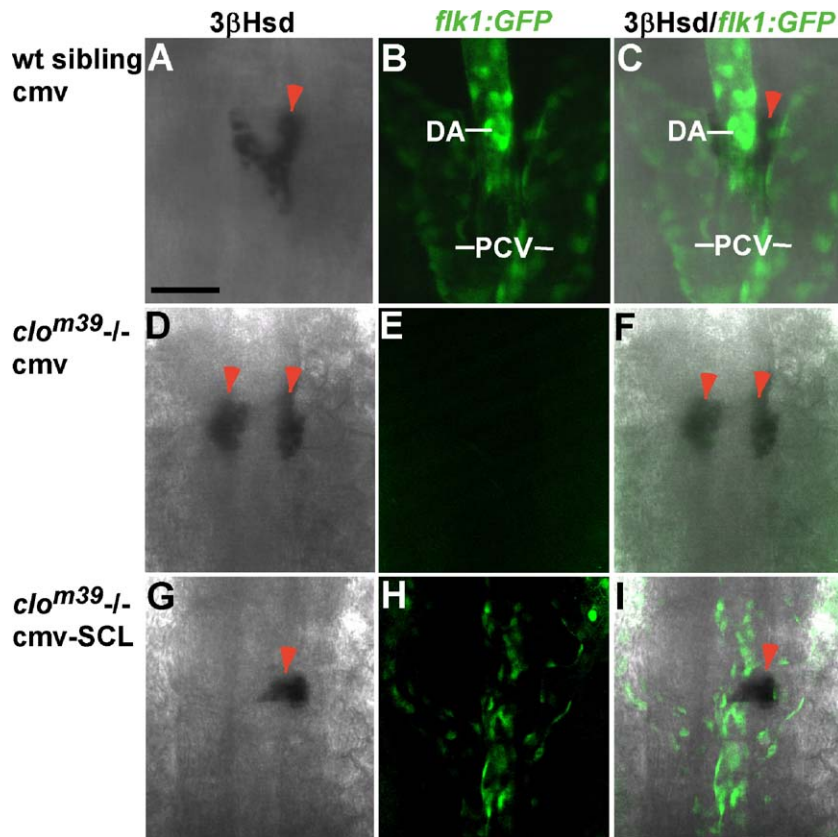

Fig. 9. Effects of forced expression of SCL on the trunk endothelium and interrenal tissue in $Tg(flk1:EGFP)^{s843}$;clo^{m39} mutants. Single confocal sections showing the interrenal tissues as detected by 3β-Hsd activity staining (Left panel: A, D, G), and the neighboring ECs as revealed by green fluorescence from $Tg(flk1:EGFP)^{s843}$ background (B, E, H), of 78 hpf homozygous clo^{m39} mutants (D–I) and their wild-type siblings (A–C), injected either with pCS2+ plasmid control (cmv; A–F) or pCS2+SCL (cmv-SCL; G–I). The merged images of 3β-Hsd activity staining and GFP are shown in the right panel (C, F, I). All panels are dorsal views with anterior oriented to the top. The trunk vasculature as well as interrenal phenotypes of wild-type siblings being injected with cmv-SCL were essentially not varying from those injected with cmv, and are hence not shown. The defective fusion of bilateral interrenal primordia in clo^{m39} is alleviated while the trunk endothelium is partially rescued. DA, dorsal aorta; PCV, posterior cardinal vein. Red arrowheads indicate interrenal tissues. Scale bar, 50 μM.

well as their wild-type sibling controls, were summarized in Table 1. Consistent with the previous studies, part of the homozygous $Tg(flk1:EGFP)^{s843};clo^{m39}$ embryos injected with *scl*-plasmids in our experiments displayed clear rescue of *flk1*-driven GFP fluorescence near the interrenal tissue (27.5%, n of $clo^{m39-/-}$ = 193), while the homozygous mutants were screened based on the enlarged heart phenotype characteristic of *clo* at 3 dpf. The rescued ECs in the mid-trunk region of *scl*-injected $Tg(flk1:EGFP)^{s843};clo^{m39}$ embryos appeared to be committed to vessel assembly at midline, although the structure of axial vessels was hypomorphic as compared with the wild type sibling controls (Figs. 9B, C, H, I). No visible rescue of EC-specific fluorescence was observed as the homozygous $Tg(flk1:EGFP)^{s843};clo^{m39}$ embryos were injected with the control plasmids (*n* = 41, Figs. 9E, F). Neither *scl*-expression nor control plasmids led to any notable perturbation of trunk vessel assembly as injected into the wild-type siblings of clo^{m39}. As shown in Table 1, defective central migration and convergence of interrenal primordia was found in 74% (103/140) of the homozygous $Tg(flk1:EGFP)^{s843};clo^{m39}$ mutants showing no rescue of trunk ECs after *scl*-plasmid injections, and in 71% (29/41) of the mutants injected with control plasmids. The penetrance was however reduced to 26% (14/53) in the homozygous $Tg(flk1:EGFP)^{s843};clo^{m39}$ mutants with clear rescue of endothelium near interrenal region by the SCL overexpression. It is thus concluded that the fusion of bilateral interrenal primordia may be dependant on the presence of neighboring ECs. The successfully-merged interrenal tissues in EC-rescued $Tg(flk1:EGFP)^{s843};clo^{m39}$ mutants were reduced in size without displaying the characteristic V-shape structure for a 3 dpf embryo (Figs. 9G, I). This might be either correlated with a hypomorphic vascular assembly near midline, or due to growth perturbations in the clo^{m39} mutants. There was no visible blood circulation established in the EC-rescued $Tg(flk1:EGFP)^{s843};clo^{m39}$ embryos, although the expressions of hematopoietic markers await to be examined. Nevertheless, blood precursors, rescued at any extent in the *scl*-injected clo^{m39} mutants, were not expected to be involved in the alleviation of interrenal migration defects, as judged from the results shown in *scl* morphants (Fig. 8). In summary, our results support that the migration defects of interrenal tissues in clo^{m39} mutant are secondary to the absence of ECs adjacent to early interrenal primordia.

Discussion

We have employed several in vivo approaches in this study to illustrate the role of ECs in promoting proper morphogenetic movement of interrenal tissue, prior to the initiation of vascular function. Firstly, migrating angioblasts and nascent vasculature were shown to be tightly associated with interrenal cells, shortly after the specification of interrenal primordia. The deletion of ECs in clo^{m39} mutant was correlated with the failed convergence of bilateral interrenal primordia at midline. Based on this observation, we have further demonstrated that the interrenal phenotype in the absence of EC was independent of defects in either vascular function or vessel formation. Rescue of trunk

endothelium in clo^{m39}, by the forced expression of SCL, led to the alleviation of interrenal migration phenotype, suggesting that the defects are secondary to the EC deficiency in clo^{m39}. Thus, an inductive role of EC precursors for the morphogenetic movement of early interrenal primordia is implied, which appeared to be disrupted in the EC-free trunk region of clo^{m39}. However, it remains unknown whether *clo* was expressed at interrenal tissue or its neighboring cells, and the availability of *clo* gene sequence will be required to address this question. Additional verifications could be performed by transplantation studies to test whether an autonomous function of *clo* at interrenal tissue could account for the interrenal migration defects in clo^{m39}. However, *clo* is required for the differentiation of all endothelial precursors in a cell-autonomous manner (Stainier et al., 1995; Parker and Stainier, 1999). Thus, any autonomous *clo* effect generated by interrenal cells per se will not be distinguishable from the activity of ECs that are rescued in transplantation assays. The issue could be clarified provided that the hemangioblast vs. pronephros/interrenal lineages could be specifically grafted from donor embryos.

Endothelial signaling in the parallel development of pronephric and interrenal primordia

Our results also suggest that the glomerular endothelium, albeit in close proximity to the developing interrenal tissue of zebrafish embryo, does not induce the midline convergence of bilateral interrenal primordia. As depicted in the diagram of Fig. 10, interrenal primordia are specified within the pronephric field at around 22 hpf, which is followed by the posterior migration out of pronephric field. In our ISH assays, no endothelium was found to be associated with interrenal cells at this stage (results not shown). After interrenal primordia are partially separated from the pronephros at around 24–24.5 hpf, their central migration toward midline is initiated. Although our results suggest that the EC clusters associated with bilateral interrenal primordia could be involved in the trunk vasculature formation, it is not clear whether they are differentiated into either arterial- or venous-fate at this stage. The *wt1*-expressing pronephric promordia do not appear to be invaded by ECs at around 24 hpf. The central migration and fusion of pronephric primordia starts later at about 30 hpf, and is temporally correlated with the angiogenesis of glomerulus. In mice, the reciprocal interaction between epithelial ureteric bud and metanephric mesenchyme requires the induction of Vegfa by Wt1 in mesenchyme, which functions by maintaining the expression of Gdnf and Pax2 (Gao et al., 2005). It remains unclear whether Wt1 exerted a similar function in inducing angiogenesis in the zebrafish pronephros. Nevertheless, the interrenal primordia-associated angioblasts at 24.5 hpf were located clearly outside of the *wt1*-expressing domain, ruling out the possibilities for them to be regulated by Wt1. The ECs invading pronephros by sprouting of dorsal aorta are regulated by blood flow to express matrix-metalloproteinase-2, which then mediate the podocyte assembly into a glomerulus (Serluca et al., 2002). In summary, the differential endothelium-derived signals that modulate interrenal vs. pronephric
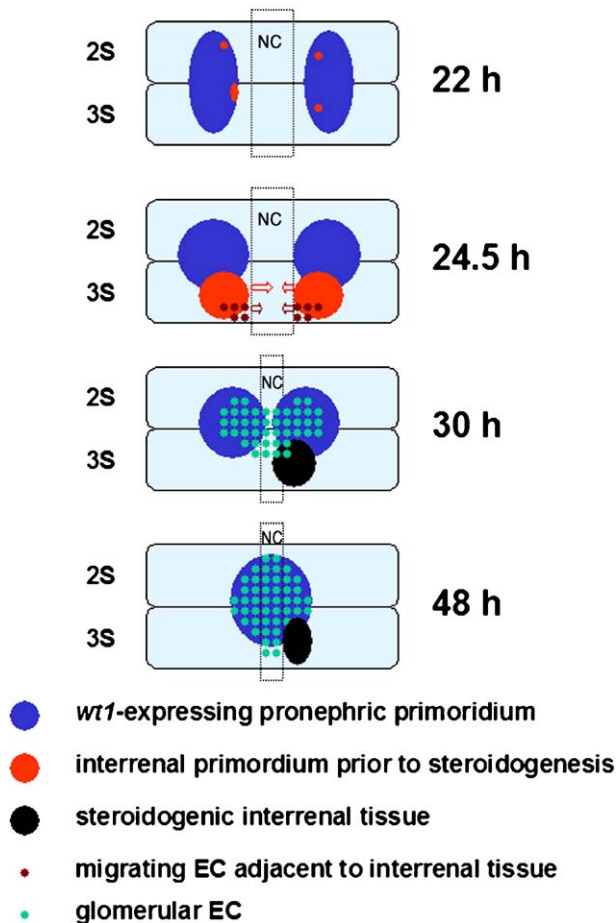
Fig. 10. The early morphogenetic movement of interrenal tissue is guided by ECs. The parallel migrations of interrenal tissue and pronephros in this schematic are depicted based on the results of this study and Hsu et al. (2003). The panels represent dorsal top views of embryos, at the indicated stages, oriented with anterior to the top. The earliest association of interrenal tissue with ECs was detected at 24.5 hpf by ISH, while no interrenal-EC interaction was detected at 22 hpf, when the primitive interrenal cell clusters resided in the pronephric field. The steroidogenesis of interrenal tissue, after migration and convergence, is correlated temporally with the angiogenesis of pronephros. The assembly of axial vasculature near pronephric-interrenal region is omitted from this diagram. NC, notochord; 2S and 3S, the second and third somite, respectively.

morphogenesis are mediated by different subsets of ECs, implying that the trunk ECs in various microenvironments could display heterogeneity in terms of their guiding functions in organ formation.

Mutual signaling between EC and interrenal tissue during development

The intimate interactions between ECs and interrenal tissues imply a paracrine nature of the endothelial signal(s), which awaits future investigations. Identified EC-derived signals have been demonstrated to mediate a diversity of biological processes including differentiation, morphogenesis, cell survival, and chemoattraction, as well as inflammation (reviewed in Cleaver and Melton, 2003; Lammert et al., 2003). For example, PDGF-BB and TGF-β are expressed by ECs to regulate the recruitment

and differentiation of mural cell progenitors, respectively, during vascular wall assembly (Leveen et al., 1994; Lindahl et al., 1997; Hirschi et al., 1998). *clo* mutant has been found to lack adrenomedullin receptor (Sumanas et al., 2005), which belongs to the family of G-coupled receptors, and is expressed in lateral mesoderm and vascular ECs in early zebrafish embryo. Adrenomedullin is a multifunctional peptide initially isolated from human pheochromocytoma, with the major effects displayed on the regulation of circulation and the homeostatic control of fluid and electrolytes (Hinson et al., 2000; Smith and Ferguson, 2001). Multiple adrenomedullin genes have been found in teleosts to be widely distributed in different tissues including the kidney and interrenal, and their functions remain to be characterized (Ogoshi et al., 2003). In zebrafish, adrenomedullin receptor appears to be regulated by *clo* at a stage well before vessel assembly (Sumanas et al., 2005). Therefore, although the signaling through adrenomedullin and its receptor appears to be most prominent in the established vessels, it might be interesting to explore its role in the migrating angioblasts, as well as in those organs that are developing with nascent vasculature in a parallel manner. Apart from adrenomedullin receptor, a complement receptor C1qR-like receptor which contains C-type lectin and calcium binding epidermal growth factor-like homology domain also displays vascular-specific expression which is down-regulated in *clo* (Sumanas et al., 2005), implying that EC-derived signaling molecules may act downstream of a key regulator of EC development, such as *clo*. Characterizations of such *clo*-regulated EC signaling molecules might shed some light on the nature of paracrine controls that mediate early interrenal-EC interactions.

It would also be intriguing to explore the properties of reciprocal signaling from early interrenal tissue, before the onset of steroidogenesis. However, the complete ablation of early interrenal tissues through the knockdown of Ff1b protein did not seem to affect the morphology of adjacent axial vessels (results not shown). It is thus speculated that the reciprocal signals may be restrictively exerted to those ECs that have invaded interrenal tissue. This would imply that the mutual signaling might initiate as late as 3 dpf, when the EC invagination appears to be evident, which might be induced by signaling molecules with equivalent functions of the mammalian EG-VEGF (LeCouter et al., 2001). Our results do not support a role for ECs in the initial differentiation of interrenal tissue, which is not to rule out the possibility that they may later exert paracrine function and induce the release of steroid(s). Specifically from what we have learned about the early interaction between EC and interrenal tissues, it remains to be defined how the morphology, intercellular adhesion, and protein expression profiles of early interrenal cells are changed in *clo*, such that we can understand the transduction mechanisms underlying the midline convergence elicited by EC-derived signals.

In summary, the evidences of this study point to a morphogenetic role of ECs, independent of either vascular formation or circulation, for the midline convergence of interrenal tissue in zebrafish. It is thus suggested that ECs, apart from their well-known functions in the differentiation and

secretion of endocrine tissues, are also required for the proper formation of endocrine organ primordia.

References

Bartman, T., Walsh, E.C., Wen, K.K., McKane, M., Ren, J., Alexander, J., Rubenstein, P.A., Stainier, D.Y., 2004. Early myocardial function affects endocardial cushion development in zebrafish. PLoS Biol. 2, 673–681.

Chai, C., Liu, Y.W., Chan, W.K., 2003. ff1b is required for the development of steroidogenic component of the zebrafish interrenal organ. Dev. Biol. 260, 226–244.

Cleaver, O., Melton, D.A., 2003. Endothelial signaling during development. Nat. Med. 9, 661–668.

Davidson, A.J., Zon, L.I., 2004. The 'definitive' (and 'primitive') guide to zebrafish hematopoiesis. Oncogene 23, 7233–7246.

Dooley, K.A., Davidson, A.J., Zon, L.I., 2005. Zebrafish scl functions independently in hematopoietic and endothelial development. Dev. Biol. 277, 522–536.

Drummond, I.A., 2003. Making a zebrafish kidney: a tale of two tubes. Trends Cell Biol. 13, 357–365.

Drummond, I.A., 2005. Kidney development and disease in the zebrafish. J. Am. Soc. Nephrol. 16, 299–304.

Field, H.A., Dong, P.D., Beis, D., Stainier, D.Y., 2003a. Formation of the digestive system in zebrafish: II. Pancreas morphogenesis. Dev. Biol. 261, 197–208.

Field, H.A., Ober, E.A., Roeser, T., Stainier, D.Y., 2003b. Formation of the digestive system in zebrafish: I. Liver morphogenesis. Dev. Biol. 253, 279–290.

Fouquet, B., Weinstein, B.M., Serluca, F.C., Fishman, M.C., 1997. Vessel patterning in the embryo of the zebrafish: guidance by notochord. Dev. Biol. 183, 37–48.

Gao, X., Chen, X., Taglienti, M., Rumballe, B., Little, M.H., Kreidberg, J.A., 2005. Angioblast-mesenchyme induction of early kidney development is mediated by Wt1 and Vegfa. Development 132, 5437–5449.

Grassi Milano, E., Basari, F., Chimenti, C., 1997. Adrenocortical and adrenomedullary homologs in eight species of adult and developing teleosts: morphology, histology, and immunohistochemistry. Gen. Comp. Endocrinol. 108, 483–496.

Green, T., 1996. Haematopoiesis. Master regulator unmasked. Nature 383, 575–577.

Gut, P., Huber, K., Lohr, J., Bruhl, B., Oberle, S., Treier, M., Ernsberger, U., Kalcheim, C., Unsicker, K., 2005. Lack of an adrenal cortex in Sf1 mutant mice is compatible with the generation and differentiation of chromaffin cells. Development 132, 4611–4619.

Hanke, C.J., Campbell, W.B., 2000. Endothelial cell nitric oxide inhibits aldosterone synthesis in zona glomerulosa cells: modulation by oxygen. Am. J. Physiol.: Endocrinol. Metab. 279, E846–E854.

Hinson, J.P., Kapas, S., Smith, D.M., 2000. Adrenomedullin, a multifunctional regulatory peptide. Endocr. Rev. 21, 138–167.

Hirschi, K.K., Rohovsky, S.A., D'Amore, P.A., 1998. PDGF, TGF-beta, and heterotypic cell–cell interactions mediate endothelial cell-induced recruitment of 10T1/2 cells and their differentiation to a smooth muscle fate. J. Cell Biol. 141, 805–814.

Hsu, H.J., Lin, G., Chung, B.C., 2003. Parallel early development of zebrafish interrenal glands and pronephros: differential control by wt1 and ff1b. Development 130, 2107–2116.

Jin, S.W., Beis, D., Mitchell, T., Chen, J.N., Stainier, D.Y., 2005. Cellular and molecular analyses of vascular tube and lumen formation in zebrafish. Development 132, 5199–5209.

Kimmel, C.B., Ballard, W.W., Kimmer, S.R., Ullmann, B., Schilling, T.F., 1995. Stages of embryonic development of the zebrafish. Dev. Dyn. 203, 253–310.

Lammert, E., Cleaver, O., Melton, D., 2001. Induction of pancreatic differentiation by signals from blood vessels. Science 294, 564–567.

Lammert, E., Cleaver, O., Melton, D., 2003. Role of endothelial cells in early pancreas and liver development. Mech. Dev. 120, 59–64.

Lawson, N.D., Weinstein, B.M., 2002. In vivo imaging of embryonic vascular development using transgenic zebrafish. Dev. Biol. 248, 307–318.

LeCouter, J., Kowalski, J., Foster, J., Hass, P., Zhang, Z., Dillard-Telm, L., Frantz, G., Rangell, L., DeGuzman, L., Keller, G.A., Peale, F., Gurney, A., Hillan, K.J., Ferrara, N., 2001. Identification of an angiogenic mitogen selective for endocrine gland endothelium. Nature 412, 877–884.

LeCouter, J., Moritz, D.R., Li, B., Phillips, G.L., Liang, X.H., Gerber, H.P., Hillan, K.J., Ferrara, N., 2003. Angiogenesis-independent endothelial protection of liver: role of VEGFR-1. Science 299, 890–893.

Leveen, P., Pekny, M., Gebre-Medhin, S., Swolin, B., Larsson, E., Betsholtz, C., 1994. Mice deficient for PDGF B show renal, cardiovascular, and hematological abnormalities. Genes Dev. 8, 1875–1887.

Liao, W., Bisgrove, B.W., Sawyer, H., Hug, B., Bell, B., Peters, K., Grunwald, D.J., Stainier, D.Y., 1997. The zebrafish gene cloche acts upstream of a flk-1 homologue to regulate endothelial cell differentiation. Development 124, 381–389.

Liao, E.C., Paw, B.H., Oates, A.C., Pratt, S.J., Postlethwait, J.H., Zon, L.I., 1998. SCL/Tal-1 transcription factor acts downstream of cloche to specify hematopoietic and vascular progenitors in zebrafish. Genes Dev. 12, 621–626.

Lindahl, P., Johansson, B.R., Leveen, P., Betsholtz, C., 1997. Pericyte loss and microaneurysm formation in PDGF-B-deficient mice. Science 277, 242–245.

Liu, Y.W., Gao, W., The, H.L., Tan, J.H., Chan, W.K., 2003. Prox1 is a novel coregulator of Ff1b and is involved in the embryonic development of the zebra fish interrenal primordium. Mol. Cell. Biol. 23, 7243–7255.

Majumdar, A., Drummond, I.A., 1999. Podocyte differentiation in the absence of endothelial cells as revealed in the zebrafish avascular mutant, cloche. Dev. Genet. 24, 220–229.

Matsumoto, K., Yoshitomi, H., Rossant, J., Zaret, K.S., 2001. Liver organogenesis promoted by endothelial cells prior to vascular function. Science 294, 559–563.

Mizrachi, Y., Naranjo, J.R., Levi, B.Z., Pollard, H.B., Lelkes, P.I., 1990. PC12 cells differentiate into chromaffin cell-like phenotype in coculture with adrenal medullary endothelial cells. Proc. Natl. Acad. Sci. U. S. A. 87, 6161–6165.

Nasevicius, A., Larson, J., Ekker, S.C., 2000. Distinct requirements for zebrafish angiogenesis revealed by a VEGF-A morphant. Yeast 17, 294–301.

Nikolova, G., Lammert, E., 2003. Interdependent development of blood vessels and organs. Cell Tissue Res. 314, 33–42.

Ogoshi, M., Inoue, K., Takei, Y., 2003. Identification of a novel adrenomedullin gene family in teleost fish. Biochem. Biophys. Res. Commun. 311, 1072–1077.

Parker, L., Stainier, D.Y., 1999. Cell-autonomous and non-autonomous requirements for the zebrafish gene cloche in hematopoiesis. Development 126, 2643–2651.

Patterson, L.J., Gering, M., Patient, R., 2005. Scl is required for dorsal aorta as well as blood formation in zebrafish embryos. Blood 105, 3502–3511.

Porcher, C., Liao, E.C., Fujiwara, Y., Zon, L.I., Orkin, S.H., 1999. Specification of hematopoietic and vascular development by the bHLH transcription factor SCL without direct DNA binding. Development 126, 4603–4615.

Reid, S.G., Fritsche, R., Jonsson, A.C., 1995. Immunohistochemical localization of bioactive peptides and amines associated with the chromaffin tissue of five species of fish. Cell Tissue Res. 280, 499–512.

Rosolowsky, L.J., Hanke, C.J., Campbell, W.B., 1999. Adrenal capillary endothelial cells stimulate aldosterone release through a protein that is distinct from endothelin. Endocrinology 140, 4411–4418.

Sehnert, A.J., Huq, A., Weinstein, B.M., Walker, C., Fishman, M., Stainier, D.Y., 2002. Cardiac troponin T is essential in sarcomere assembly and cardiac contractility. Nat. Genet. 31, 106–110.

Serluca, F.C., Drummond, I.A., Fishman, M.C., 2002. Endothelial signaling in kidney morphogenesis: a role for hemodynamic forces. Curr. Biol. 12, 492–497.

Shalaby, F., Rossant, J., Yamaguchi, T.P., Gertsenstein, M., Wu, X.F., Breitman, M.L., Schuh, A.C., 1995. Failure of blood-island formation and vasculogenesis in Flk-1-deficient mice. Nature 376, 62–66.

Shalaby, F., Ho, J., Stanford, W.L., Fischer, K.D., Schuh, A.C., Schwartz, L., Bernstein, A., Rossant, J., 1997. A requirement for Flk1 in primitive and definitive hematopoiesis and vasculogenesis. Cell 89, 981–990.

Shivdasani, R.A., Orkin, S.H., 1996. The transcriptional control of hematopoiesis. Blood 87, 4025–4039.

Smith, P.M., Ferguson, A.V., 2001. Adrenomedullin acts in the rat paraventricular nucleus to decrease blood pressure. J. Neuroendocrinol. 13, 467–471.

Stainier, D.Y., Weinstein, B.M., Detrich III, H.W., Zon, L.I., Fishman, M.C., 1995. *cloche*, an early acting zebrafish gene, is required by both the endothelial and hematopoietic lineages. Development 121, 3141–3150.

Stainier, D.Y., Fouquet, B., Chen, J.N., Warren, K.S., Weinstein, B.M., Meiler, S.E., Mohideen, M.A., Neuhauss, S.C., Solnica-Krezel, L., Schier, A.F., Zwartkruis, F., Stemple, D.L., Malicki, J., Driever, W., Fishman, M.C., 1996. Mutations affecting the formation and function of the cardiovascular system in the zebrafish embryo. Development 123, 285–292.

Sumanas, S., Jorniak, T., Lin, S., 2005. Identification of novel vascular endothelial-specific genes by the microarray analysis of the zebrafish *cloche* mutants. Blood 106, 534–541.

Sumoy, L., Keasey, J.B., Dittman, T.D., Kimelman, D., 1997. A role for notochord in axial vascular development revealed by analysis of phenotype and the expression of VEGR-2 in zebrafish *flh* and *ntl* mutant embryos. Mech. Dev. 63, 15–27.

Weinstein, B.M., Schier, A.F., Abdelila, S., Malicki, J., Solnica-Krezel, L., Stemple, D.L., Stainier, D.Y., Zwartkruis, F., Driever, W., Fishman, M.C., 1996. Hematopoietic mutations in the zebrafish. Development 123, 303–309.

Westerfield, M., 2000. The Zebrafish Book: Guide for the Laboratory Use of Zebrafish (*Danio rerio*), 4th ed. Univ. Oregon Press, Eugene, OR.

Yoshitomi, H., Zaret, K.S., 2004. Endothelial cell interactions initiate dorsal pancreas development by selectively inducing the transcription factor Ptf1a. Development 131, 807–817.

Zhong, T.P., Rosenberg, M., Mohideen, M.A., Weinstein, B., Fishman, M.C., 2000. *gridlock*, an HLH gene required for assembly of the aorta in zebrafish. Science 287, 1820–1824.

Zhong, T.P., Childs, S., Leu, J.P., Fishman, M.C., 2001. Gridlock signalling pathway fashions the first embryonic artery. Nature 414, 216–220.